Research Journal of Applied Sciences, Engineering and Technology 6(22): 4271-4280, 2013
ISSN: 2040-7459; e-ISSN: 2040-7467

Submitted: March 06, 2013 Accepted: April 02, 2013 Published: December 05, 2013

A Differential Evolution Based Adaptive Neural Network Pitch Controller for a Doubly Fed Wind Turbine Generator System

[1]A.H.M.A. Rahim and [2]Syed A. Raza
[1]Department of Electrical Engineering, King Fahd University of Petroleum and Minerals, Dhahran 31261, Saudi Arabia
[2]Department of Electrical Engineering, Prince Mohammad Bin Fahd University, Al-Khobar, Saudi Arabia

Abstract: Extraction of maximum energy from wind and transferring it to the grid with high efficiency are challenging problems. To this end, this study proposes a smart pitch controller for a wind turbine-doubly fed induction generator system using a Differential Evolution (DE) based adaptive neural network. The nominal weights for the back-propagation neural network controller are obtained from input-output training data generated by DE optimization method. These weights are then adaptively updated in time domain depending on the variation of the system outputs. The adaptive control strategy has been tested through simulation of complete system dynamics comprising of the turbine-generator system and its various components. It has been observed that the DE based smart pitch controller is able to achieve efficient energy transfer to the grid and at the same time provide a good damping profile. Locally collected wind data was used in the testing phase.

Keywords: Adaptive pitch control, back-propagation neural network, differential evolution, doubly fed generator, wind turbine

INTRODUCTION

Most modern wind turbines used in utility are the variable speed Doubly Fed Induction Generator (DFIG) or Permanent Magnet Synchronous Generator (PMSG) types. Although costly power electronics are required to convert power at varying frequency, the variable speed wind turbines are industry favorite because of their better energy capture capability, operation at higher efficiency and lower loading (Muljadi and Butterfield, 2001). When compared with the synchronous generator type, the DFIG wind turbine have additional advantage in terms of reduced converter losses, independent real and reactive power control, grid support through reactive control etc. (Lin *et al*., 2011a) The utility-scale turbines generally have three levels of control, the uppermost is supervisory control, mid-level turbine control and in the lowest level are the pitch actuator control, the generator and power electronics control (Johnson *et al*., 2006).

A major disadvantage of the induction type wind generators is their sensitivity to low voltage conditions at the grid. Fault ride of DFIG is a matter of intense research in the recent times. Various types of controls on the converter system have been attempted by several investigators. Reference (Vinothkumar and Selvan, 2011) presents an interesting strategy of low voltage ride using a circuit comprising of a rectifier and IGBT in the rotor side converter and inductor in parallel with it. Voltage source inverter with current controller was employed by Muyeen *et al*. (2011) for fault ride through. Hybrid current controllers in the converter circuit has been used for improving fault ride through capabilities which comprises of a standard PI controller in addition to hysteresis current controller (Mohseni *et al*., 2011). A voltage source converter connected between the generator and grid, termed a voltage restorer and a virtual resistance deactivating the normal crowbar has been employed for riding low voltages (Ibrahim *et al*., 2011; Hu *et al*., 2011). Use of FACTS (flexible ac transmission system) and energy storage devices which supply both real and reactive power have the additional advantage that they also provide damping to the system during the low voltage recovery. The devices which have been used to enhance the wind system performance vary from simple static VAR controller (Amaris and Alonso, 2011), battery energy storage (Mendis *et al*., 2012), supercapacitor with STATCOM (Qu and Qiao, 2011; Rahim and Nowicki, 2012), etc. Superconducting magnetic energy storage (SMES) units can be controlled to supply both real and reactive power and are shown to be effective in terms of leveling wind power fluctuations as well as low voltage ride through (Shi *et al*., 2011; Yunus *et al*., 2012).

The inertia of the turbine-generator rotor is large and hence the rotor speed control is relatively slow. The

Corresponding Author: A.H.M.A. Rahim, Department of Electrical Engineering, King Fahd University of Petroleum and Minerals, Dhahran 31261, Saudi Arabia, Tel.: +96638604986

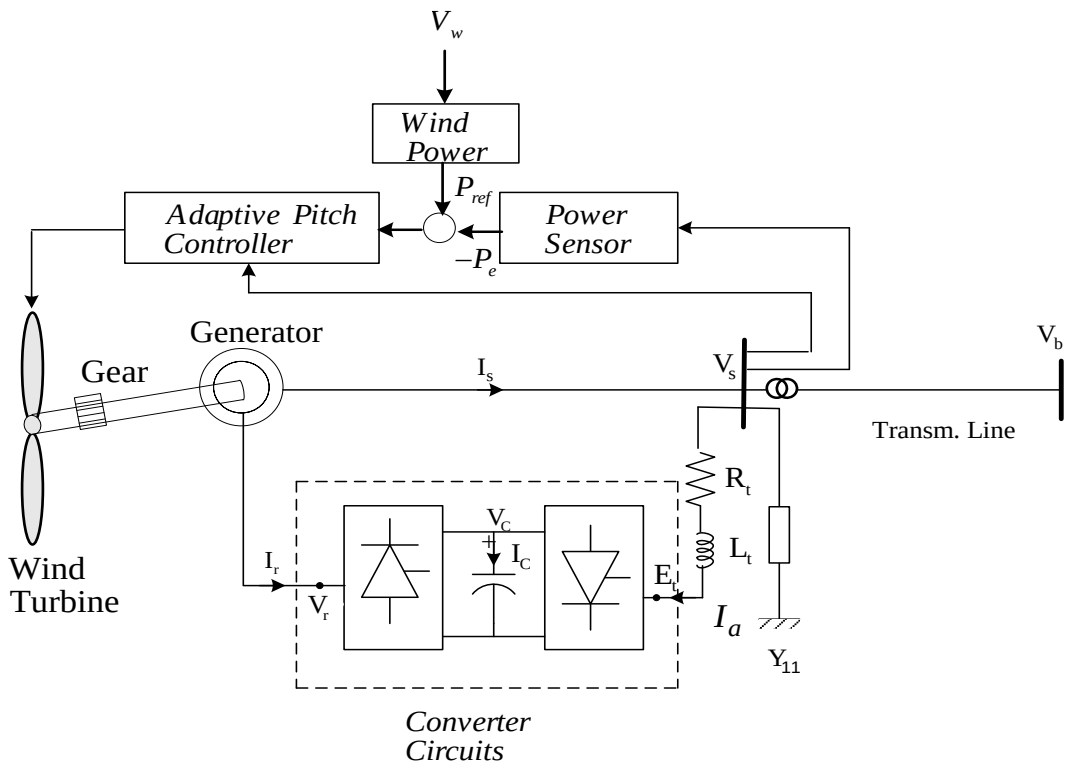

Fig. 1: DFIG system configuration equipped with pitch controller

doubly fed generator based wind plants do not have good frequency response characteristics because of lack of coupling between grid frequency and output power. Also, the DFIG does not have reserve margin in maximum power tracking (Zhang *et al*., 2012). Since pitch control is relatively faster the aerodynamic power can be regulated to limit rotor speed (Muljadi and Butterfield, 2001). Generally, nonlinear strategies are involved for power maximization and also for frequency regulation analysis (Moutis *et al*., 2012). A PI (proportional integral) controller has been used for generator and pitch actuators using small-signal analysis in Riziotis *et al*. (2008). Maximum energy capture using PI and fuzzy logic controllers were proposed in Kamel *et al*. (2011) and Lin *et al*. (2011b). Reference (Kamel *et al*., 2011) uses PI controllers in battery storage system, while (Lin *et al*., 2011b) employs a fuzzy interface to estimate the wind speed fluctuations. Applications of intelligent techniques for maximizing energy capture have been reported in the literature in recent times. Pitch control to regulate the output power of squirrel cage type wind generator through neural network was reported in Yilmaz and Ozer (2009). The output power leveling by generalized pitch control has been used in Senjyu *et al*. (2006). Also, artificial neural network has been employed for achieving fast and stable response for a stand-alone hybrid system (Lin *et al*., 2011c).

Generally, in aerodynamic modeling and pitch control studies the relatively slower rotor dynamics is considered. Since the generator wheels the energy, its dynamics should be adequately modeled. Also, because of random nature of wind variation, the any control design should include the system nonlinearities. This makes the pitch controller design difficult. In this study a smart pitch control strategy for a turbine-generator system is obtained in time domain by using an adaptive Back-Propagation (BP) neural network. The back-propagation network is used because it is known that a three layered BP can approximate any nonlinear function under any precision (Xu *et al*., 2012). The starting weights for the back-propagation network are obtained through an optimum evolutionary algorithm.

SYSTEM MODEL

A block diagram of the wind turbine-generator is given in Fig. 1. The converter circuitry of the doubly fed induction generator (DFIG) is located between the generator stator and rotor terminals. The grid connects to the stator through transformer and line. A local load is located at the generator terminal bus. The turbine has a pitch control system shown in the block diagram. The system model includes the turbine dynamics and its pitch controller, the DFIG and converter circuitry, the line and the load.

The doubly fed generator and converter model: The differential equations relating the voltage current and

flux of the stator and rotor circuit of a DFIG expressed in per unit (pu) quantities along the d-q axes are:

$$\frac{1}{\omega_0}\dot{\Psi}_{ds} - \frac{\omega_e}{\omega_0}\Psi_{qs} - R_s i_{ds} = v_{ds}$$
$$\frac{1}{\omega_0}\dot{\Psi}_{qs} + \frac{\omega_e}{\omega_0}\Psi_{ds} - R_s i_{qs} = v_{qs} \quad (1)$$

$$\frac{1}{\omega_0}\dot{\Psi}_{dr} - s\Psi_{qr} - R_r i_{dr} = v_{dr}$$
$$\frac{1}{\omega_0}\dot{\Psi}_{qr} + s\Psi_{dr} - R_s i_{qr} = v_{qr} \quad (2)$$

The relationships between the flux linkages and currents of the stator and rotor circuits are:

$$\Psi_{ds} = -x_s i_{ds} - x_m i_{dr} \qquad \Psi_{dr} = -x_r i_{dr} - x_m i_{ds}$$
$$\Psi_{qs} = -x_s i_{qs} - x_m i_{qr} \qquad \Psi_{qr} = -x_r i_{qr} - x_m i_{qs} \quad (3)$$

The slip (s) of the machine given in the above expressions is $(\omega_s - \omega_r)/\omega_s$. The input current to the converter on the grid side, written in terms of d-q components, is Rahim and Habiballah (2011):

$$\frac{d}{dt}\begin{bmatrix} i_{da} \\ i_{qa} \end{bmatrix} = \frac{\omega_0}{L_a}\begin{bmatrix} -R_a & X_a \\ -X_a & R_a \end{bmatrix} + \frac{\omega_0}{L_a}\begin{bmatrix} v_{ds} - E_{qa} \\ v_{qs} - E_{qa} \end{bmatrix} \quad (4)$$

Here, $I_a = i_{da}+ji_{qa}$, $V_s = v_{ds}+jv_{qs}$ and $E_a = e_{da}+je_{qa}$, ω_0 is the base frequency. The DC ink capacitor is located between the two back to back converters. Neglecting the power loss in the capacitor, the power balance yields the following capacitor voltage equation:

$$\frac{dV_c}{dt} = \frac{1}{C}[m_1 \cos\alpha_1 i_{da} + m_1 \sin\alpha_1 i_{qa} + m_2 \cos\alpha_2 i_{dr} + m_2 \sin\alpha_2 i_{qr}] \quad (5)$$

The modulation index and phase angle of the two converter voltages on grid and rotor sides, $(m_1\ m_2)$ and $(\alpha_1\ \alpha_2)$, relate to the DC capacitor voltage V_c through:

$$E_{da} = m_1 V_c \cos\alpha_1 \qquad v_{dr} = m_2 V_c \cos\alpha_2$$
$$E_{qa} = m_1 V_c \sin\alpha_1 \qquad v_{qr} = m_2 V_c \sin\alpha_2 \quad (6)$$

Aerodynamics and drive model: The rotor drive train model for the turbine-generator system in terms of torsional angle between the two masses and their speed are expressed as:

$$\dot{\omega}_t = \frac{1}{2H_t}[P_m - K_s\theta_s]$$
$$\dot{\theta}_s = \omega_e[\omega_t - \omega_r]$$
$$\Delta\dot{\omega}_r = \frac{1}{2H_g}[K_s\theta_s - P_e] \quad (7)$$

The mechanical input power, which is the turbine output, is:

$$P_m = \frac{1}{2}\gamma\pi R^2 V_w^3 C_p(\lambda,\alpha) \quad (8)$$

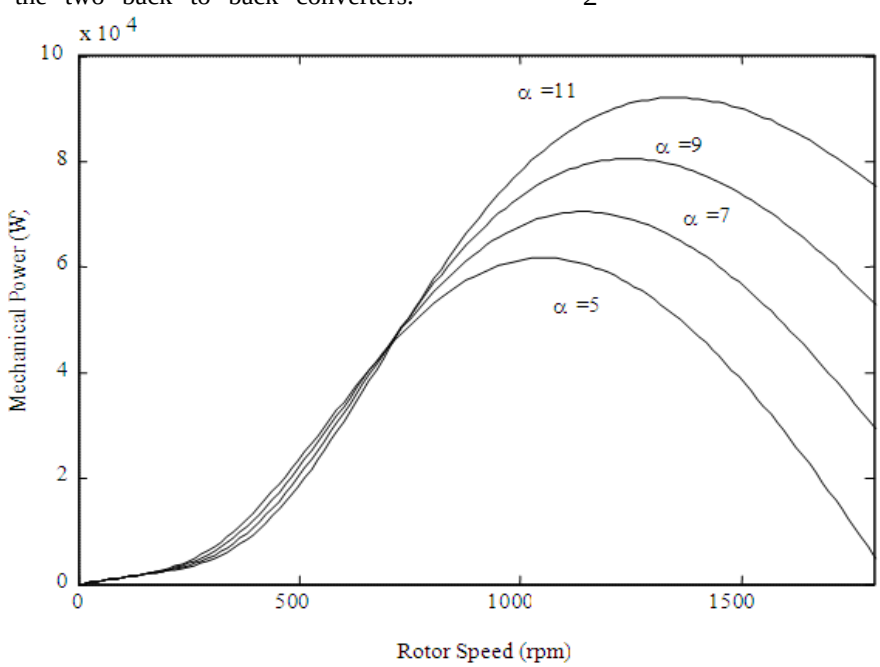

Fig. 2: Mechanical power for various pitch angles at wind speed of 12 m/s

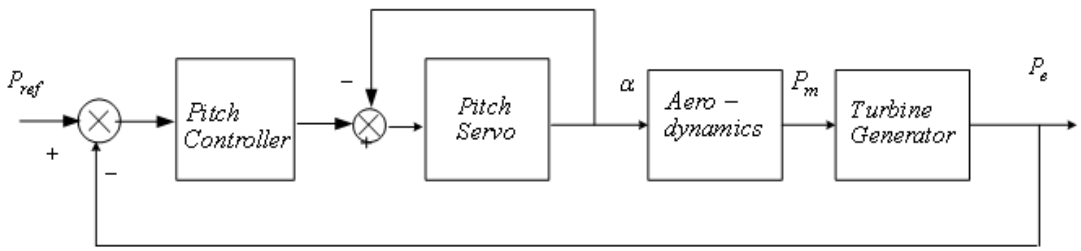

Fig. 3: Pitch controller block diagram

Here, V_w, γ, λ, C_p, α are the wind velocity, tip speed ratio, density of air, power coefficient and pitch angle, respectively. C_p depends λ and α through the highly non-linear relationship:

$$C\beta_p(\lambda,\beta) = 0.5176\left[\frac{116}{\lambda_i} - 0.4 \quad -5\right]e^{\frac{-21}{\lambda_i}} + 0.0068\lambda$$
$$\frac{1}{\lambda_i} = \frac{1}{\lambda + 0.08\alpha} - \frac{0.035}{\alpha^3 + 1} \tag{9}$$

The electrical power output term in (7) is given as:

$$P_e = \Psi_{qr} i_{dr} - \Psi_{dr} i_{qr} \tag{10}$$

Plot of the turbine power output against generator speed for wind speed of 12m/s is given in Fig. 2 for different pitch angles.

Pitch controller: Figure 3 presents the block diagram of the pitch controller system. The pitch controller is actuated between the reference and actual output of the generator. From (8) and (9) it can be seen that the input power to the generator can be controlled through control of pitch angle α. The blade pitch angle depends on control of the pitch servos. The pitch servo system model includes a rate limiter, an angle limiter, delay elements, etc. Conventionally a pitch angle control system uses PI controllers to generate the appropriate α. While a more detailed servo modeling may be used, a first order servo system is sufficient in investigations of power system studies. In this study, all the components in the pitch control and servo system are included in the parameters of the PI controller, dynamic relationships of which are:

$$\dot{\gamma} = K_I \Delta P$$
$$\dot{\alpha} = K_P \Delta P + \gamma \tag{11}$$

Here, K_P and K_I are the controller gains to be determined; ΔP is the input to the controller and α is the pitch angle.

The composite model of the turbine-generator system which includes the pitch control device is expressed through the state model:

$$\dot{x} = f[x, u]$$
$$y = g[x, u] \tag{12}$$

The input u represents the pitch controller gains and *y* is the vector of selected output variables.

ADAPTIVE BPNN BASED PITCH CONTROLLER

A block diagram of the adaptive back-propagation neural network (BPNN) based pitch controller proposed in this work is shown in Fig. 4. The core of the controller consists of two BP networks, one which produces the nominal weight and nominal control (u_{nom}) through training of a large input-output data set. This part of the controller guarantees a stable nominal bounded-input bounded output system (Suresh, 2009). The other BP network is responsible to modify the network weights in time domain depending on the wind system transients and generates control Δu. The pitch controller gains are adaptively tuned as Δu changes. A differential evolution (DE) optimization technique is employed to create the input-output data for training the nominal BPNN network. The DE optimization procedure, the back-propagation and adaptive back-propagation methods are presented briefly in the following.

Differential evolution: In training the neural network the objective function used is, generally, multimodal. The gradient technique based algorithms for such problems may end up producing a local minimum. This can be avoided by employing a global optimization procedure based on evolutionary methods. Differential Evolution (DE) is such a procedure suitable for finding global minimum (Slowik, 2011). Although initially used for a single objective function, it has the capability of handling multi-objective functions and equality as well as inequality constraints (Qin *et al*., 2010). The major steps in a DE algorithm are mutation, crossover and selection of the population. The final retention is through a check of fitness on the population. The steps in the search for the pitch control parameters are summarized below (Lu *et al*., 2011).

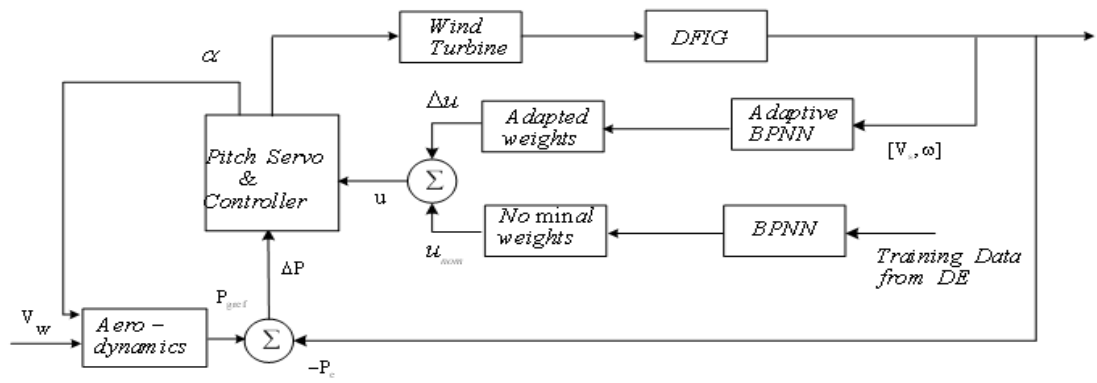

Fig. 4: Adaptive BP neural network-based pitch controller

The various steps involved in the evolutionary progression are given below:

- **Initialization:** In this step, it is required to specify the number of control variables or problem dimension with their corresponding constraints. For each control parameter, a population is generated within the search space using the relationship:

$$z_k = z_{\min} + random(z_{\max} - z_{\min}); k = [1, N_P] \quad (13)$$

In the above, N_P is total number population and N_G is the number of generations.

- **Evaluation and location of the best solution:** The best solution among the initial population is obtained from the objective function:

$$J = \sum_{k=1}^{N_P} (\xi_k - \xi_0)^2 \quad (14)$$

Here, ζ_k is the damping ratio calculated from dominant eigenvalues of the linearized system obtained from (12) for each population *k* and ζ_0 is the desired damping ratio. The objective function in (14) is minimized to provide the optimal solution satisfying all the constraints.

- **Mutation:** The mutation process aims to produce a new generation of solutions. For every individual *k*, we build a donor vector V_k from three random solutions Z_{r1}, z_{r2} and Z_{r3} among the population. The difference of any two solutions is added to the third through a mutation factor F given by the relation:

$$v_k = z_{r1} + F\left[z_{r2} - z_{r3}\right] \quad (15)$$

The limit violation in the mutant vector is checked through (14):

- **Crossover:** This is employed to have a second generation to enhance the diversity employing a binomial type crossover given by:

$$u_{k,j} = \begin{cases} v_{k,j} & \text{if } rand(0,1) < CR, \\ z_{k,j} & \text{otherwise} \end{cases} \quad (16)$$

CR represents the crossover factor.

- **Selection:** The selection process in DE involves determining survivor of a generation by comparing the trial vector with the parents based on fitness in terms of objective value (14):

$$z_k^{'} = \begin{cases} u_k & \text{if } J(u_k \le z_k) \\ z_k & \text{otherwise} \end{cases} \quad (17)$$

- **Stopping criteria:** The procedure is continued until a solution is reached within pre-specified precision or the maximum number of iteration is exceeded.

Back propagation neural network: Artificial neural networks are parallel and distributed information systems which are used to learn complex systems and generalize the information learned. The massive networks comprise of simple neurons and consist of interconnected elements called nodes. The Back-Propagation Neural Network (BPNN) considered in Fig. 4 has three layers-the Input (I), Hidden (H) and output (O) layer. The hidden layer comprises of L-1 sub-layers, the input layer being numbered 0 and output layer L. The data is transferred from input to the output node through the weight linked hidden neurons using an activation function. The activation function considered is a sigmoid having the characteristic:

$$\phi(I) = \frac{1}{1+e^{-\sigma I}}; \phi^{'}(I) = \frac{\partial \phi}{\partial x} = \sigma\phi(I)[1-\phi(I)] \quad (18)$$

The back-propagation algorithm minimizes the error function E written as:

$$E(k) = \frac{1}{2}\sum_j e_j^2(k) = \frac{1}{2}\sum_j [Od_j(k) - O_j(k)]^2 \tag{19}$$

Od_j is the desired output corresponding to j^{th} neuron and k represents the iteration count. The change in weight between the ith and j^{th} node is computed by using the gradient descent and is written as:

$$\Delta w_{ij}(k) = -\eta_1 \frac{\partial E(k)}{\partial w_{ij}} \tag{20}$$

The gradient term can be evaluated through a chain rule and the recursive relationship for the weight updates can be shown to be (Lee, 2008):

$$w_{ij}^{(l)}(k+1) = w_{ij}^{(l)}(k) + \eta_1 \gamma_j^{(l)}(k) O_i^{(l-1)}(k) + \alpha_M [w_{ij}^{(l)}(k) - w_{ij}^{(l)}(k-1)] \tag{21}$$

$$\gamma_j^l(k) = \begin{cases} e_j^{(L)} \phi_j'[H_j^{(L)}(k)] & \text{for neuron } j \text{ at output layer L} \\ \phi_j'[H_j^{(L)}(k)] \sum_m \gamma_m^{(l+1)}(k) w_{kj}^{l+1}(k) & j \text{ in hidden layer} \end{cases} \tag{22}$$

The computation is accelerated through the momentum constant α_M is the learning rate parameter η_1. Note that for $i = 0$, the weight w_{0j} corresponds to the bias at layer l_j and $H_j^{(L)} = O_j$. The back propagation algorithm has two different computational directions. In the forward direction the weights remain unchanged and the signals are computed at different nodes. The weights are updated in the backward pass from the error signal propagated backwards.

Adaptive back-propagation neural network: The back-propagation network is trained through a large input-output data set which, in turn, is generated by DE algorithm. The trained weights are then used to calculate the nominal value of controller parameters (u_{nom}) for a certain operating condition. Depending on the variation of system outputs from their desired values, the control parameters are updated as time advances according to the relation:

$$u = u_{nom} + \Delta u \tag{23}$$

The weight adaptation process is carried out by minimizing the mean square error $E_c(t)$ at each instant of time expressed as:

$$E_c(t) = \frac{1}{2}\sum_j e_c^2(t); \quad e_c(t) = r(t) - y(t) \tag{24}$$

Here, y(t) is the output vector given in (12) and r(t) is the desired output. The gradient descent method gives the change in weight:

$$\Delta w_{ij}(t) = -\eta_2 \frac{\partial E_c(k)}{\partial w_{ij}} \tag{25}$$

The weight update is obtained by adding the change with the nominal value generated by training the input-output data set and is finally expressed by:

$$w_{ij}^{(l)}(t) = w_{ij(nom)}^{(l)} + \eta_2 \gamma_j^{(l)}(t) y_i(t) \tag{26}$$

The expression for γ_j is similar to that given in (22). The output can be found from (12) or from online measurements. The nominal values of w_{ij} are assumed to remain constant during the process time.

TESTING THE ADAPTIVE PITCH CONTROLLER

The proposed adaptive pitch controller strategy was tested on the turbine-generator system of Fig. 1. The ability of the pitch control strategy to transfer the wind power under varying wind speed condition was investigated considering different wind speed conditions. The nominal power output of the DFIG at a speed of 12 m/s is 0.9 pu. The parameter values of the various components are included in the Appendix. The nominal gains of the pitch controller are considered as $K_P = 1$, $K_I = 0$. Responses with two types of wind speed variation are reported here -a step change of wind speed and random speed change as recorded at a local site.

Figure 5 to 7 show the plots of various responses for a step change in wind speed from 12 m/s to 11 m/s. The speed change is affected at t = 1s. In the absence of pitch control the wind power output at the new speed is 0.82 pu. Figure 5 shows the power input to the generator (solid line) and power output with and without adaptive pitch controller (dotted and dashed

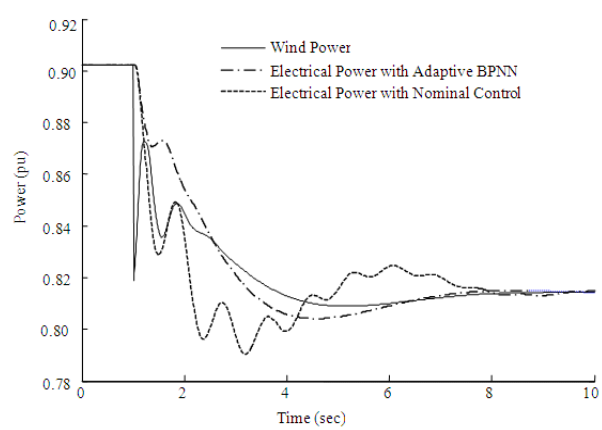

Fig. 5: Generator power input and output variation for a step decrease of wind speed by 1 m/s. The step change is made at t = 1s

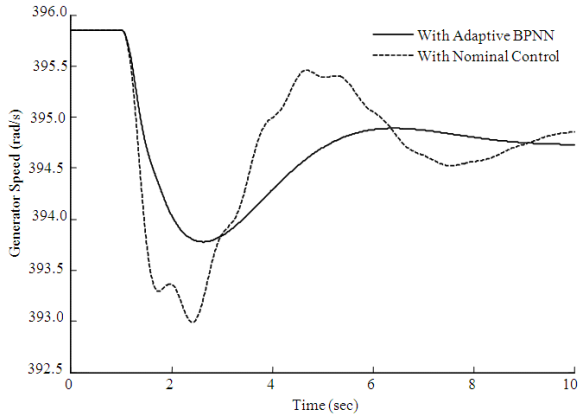

Fig. 6: Generator speed variation corresponding to Fig.5 with, (a) proposed adaptive neural network based pitch control and (b) nominal pitch control

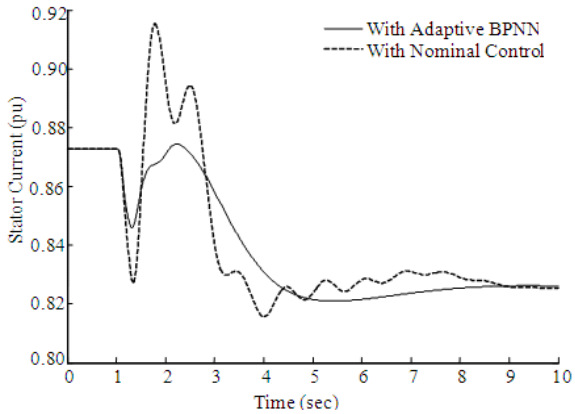

Fig. 7: DFIG stator current with a step change corresponding to Fig. 5, with (a) adaptive neural network pitch control and (b) nominal pitch control

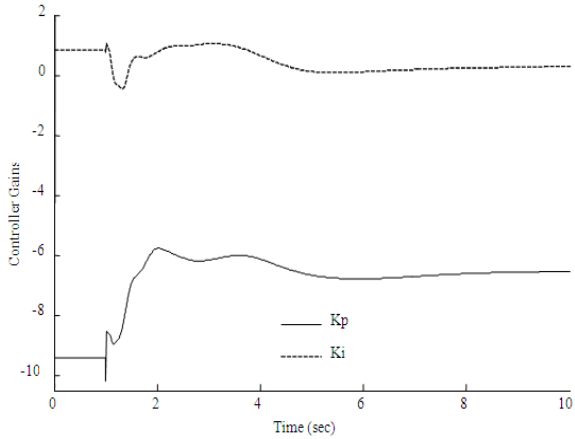

Fig. 8: Variation of PI controller gains following a step change in wind speed corresponding to Fig. 5

lines). Examination of Fig. 5 reveals that the generator output power follows the wind power very closely with the proposed adaptive neural network based control.

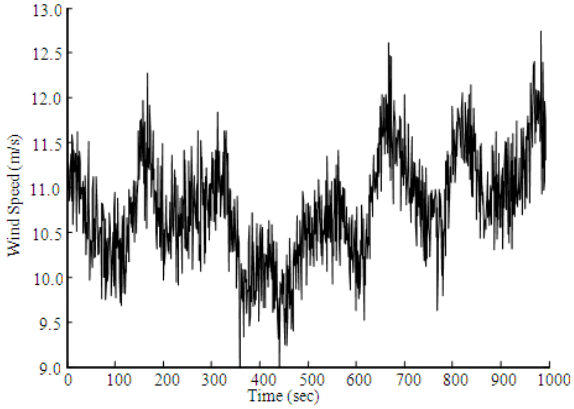

Fig. 9: Normalized wind speed record collected at the local site

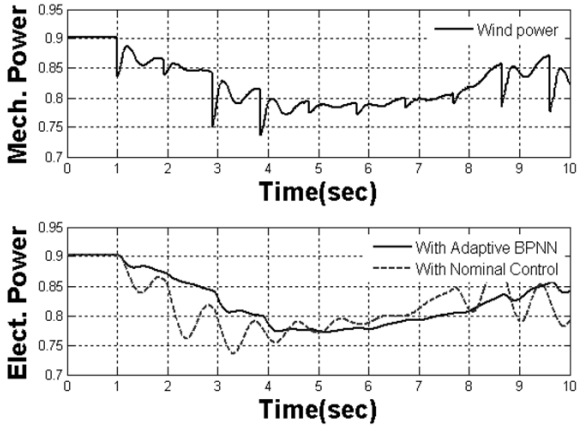

Fig. 10: Wind power and electrical power output with and without adaptive BPNN pitch control for the random wind speed variation of Fig. 9

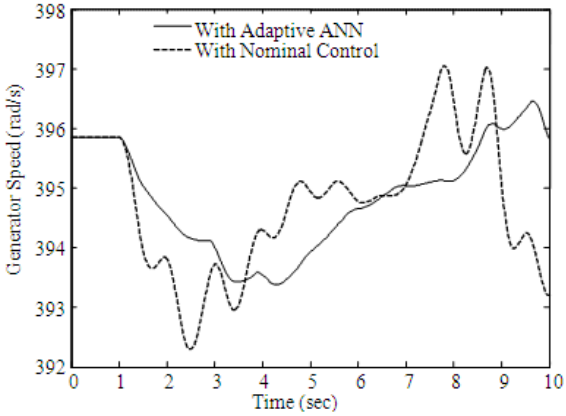

Fig. 11: Generator speed variation for random wind speed variation of Fig. 9 with, a) adaptive neural network based pitch control, b) pitch control with nominal parameters

Figure 6 and 7 show the variations of the generator speed and stator current with the proposed adaptive pitch control strategy and with nominal control. The

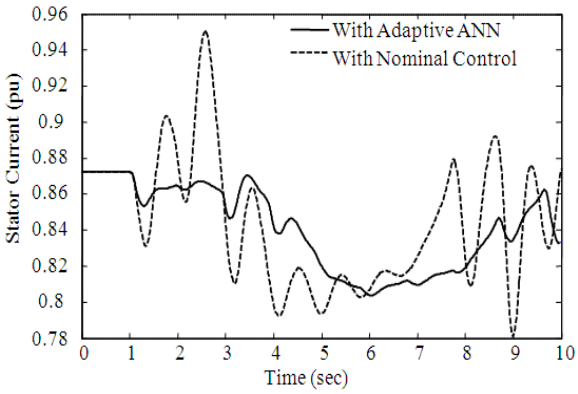

Fig. 12: Generator stator current variations with random wind speed variation with, (a) adaptive neural network based pitch control and (b) nominal pitch control

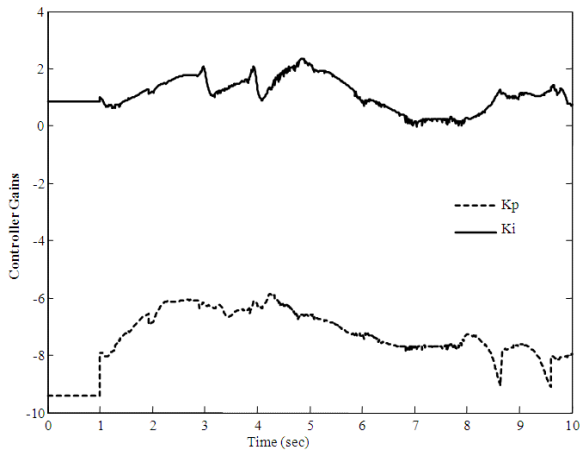

Fig. 13: Controller parameter variations with the adaptive control for the randomly changing wind speed condition of Fig. 9

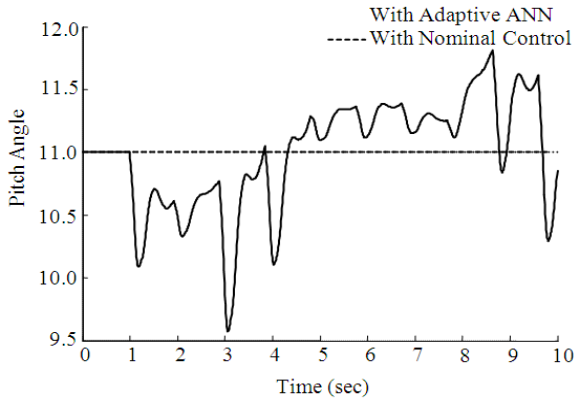

Fig. 14: Pitch angle variations with the adaptive neural network control for randomly varying wind speed changes of Fig. 9. The nominal angle is shown by the dotted line

figures indicate that the proposed control affects transfer of wind power to the grid with a very good damping profile. Figure 8 shows the variation of the controller gains during the adaptation period. Note that it is the variation of these parameters which contribute to the improved system performance.

Figure 9 shows the wind speed data recorded at the local wind generator station for a period of 1000s. The actual wind data has been normalized and scaled around a nominal value of 11 m/s. The transient responses shown in Fig. 10 to 14 are for the interval of 1s to 10s of the record of Fig. 9, wind speed kept constant at 11m/s for the first 1s. A comparison of the power input to the generator (wind power), electrical power output with the proposed adaptive pitch control and also with nominal pitch control is presented in Fig. 10. From the response it can be seen that pitch controller makes the generator output track the wind power very well. Records of generator output power, speed and stator current, shown in Fig. 10 to 12, show that the adaptive control is very effective in damping the electrical transients even for this randomly varying wind speed changes. Figure 13 shows the variation of the controller gains over the 10s period. Figure 14 shows the variation of the pitch angle during this period. It can be observed that the pitch angle change is not large during the transient period.

CONCLUSION

This study proposes a novel adaptive pitch controller for a wind turbine-DFIG system for transferring wind power to the grid efficiently. Contrary to conventional offline neural network designs, the proposed controller adapts the network weights in time domain depending on system transients. In normal maximum power transfer problems only the turbine generator rotor dynamics is considered, while this study incorporates a detailed model of the generator and its converter circuitry along with the turbine aerodynamics. The simulation results show that the neural network based pitch controller enables the electric power to follows the mechanical power closely by varying the blade pitch angle adaptively.

This is achieved with minimum transients in the generator system. The differential evolution technique used in training the neural network is an efficient method to find the global minimum. The proposed adaptive back-propagation algorithm is computationally simple.

ACKNOWLEDGEMENT

This research study was done as part of project RG 1202-1 & 1202-2 of the KFUPM research grant. The support rendered by King Fahd University of Petroleum and Minerals is gratefully acknowledged.

APPENDIX

Nomenclature and system data:

Mean wind speed (V_W)	12 m/s
Radius of the blades (R)	13.5 m
Density of air (γ)	1.225 kg/m^2
Turbine intertia (H_t)	2 s
Generator intertia (H_g)	0.5 s
Shaft stiffness (K_s)	0.3 p.u/el.rad
Stator reactance (x_s)	0.09241 p.u
Stator resistance (R_s)	0.00488 p.u
Rotor reactance (x_r)	0.2 p.u
Rotor resistance (R_r)	0.0059 p.u
Mutual inductance (x_m)	3.95379 p.u
Grid side converter resistance (R_a)	0.001 p.u
Grid side converter reactance (L_a)	0.1 p.u
Line resistance	0.02 p.u
Line reactance	0.15 p.u
DC link capacitor (C)	1.0 p.u

REFERENCES

Amaris, H. and M. Alonso, 2011. Coordinated reactive power management in power networks with wind turbines and FACTS devices. Energ. Convers. Manage., 52: 2575-2586.

Hu, S., X. Lin, Y. Kang and X. Zou, 2011. An improved low-voltage ride-through control strategy of doubly fed induction generator during grid faults. IEEE T. Power Electr., 26: 3653-3665.

Ibrahim, A.O., T.H. Nguyen, D.C. Lee and S.C. Kim, 2011. A fault ride-through technique of DFIG wind turbine systems using dynamic voltage restorers. IEEE T. Energ. Convers., 26: 871-882.

Johnson, K.E., L.Y. Pao, M.J. Balas and L.J. Fingersh, 2006. Control of variable speed wind turbines: Standard and adaptive techniques for maximizing energy capture. IEEE Control Syst. Mag., 26(3): 70-81.

Kamel, R.M., A. Chaouachi and K. Nagasaka, 2011. Enhancement of micro-grid performance during islanding mode using storage batteries and new fuzzy logic pitch angle controller. Energ. Convers. Manage., 52: 2204-2216.

Lee, T.L., 2008. Back-propagation neural network for the prediction of the short-term storm surge in Taichung harbor, Taiwan. Eng. Appl. Artif. Intell., 21: 63-72.

Lin, W.M., C.M. Hong and F.S. Cheng, 2011a. Design of intelligent controllers for wind generation system with sensorless maximum wind energy control. Energ. Convers. Manage., 52: 1086-1096.

Lin, W.M., C.M. Hong, T.C. Ou and T.M. Chiu, 2011b. Hybrid intelligent control of PMSG wind generation system using pitch angle control with RBFN. Energ. Convers. Manage., 52: 1244-1251.

Lin, W.M., C.M. Hong and C.H. Chen, 2011c. Neural-network-based MPPT control of a stand-alone hybrid power generation system. IEEE T. Power Electr., 26: 3571-3581.

Lu, Y., J. Zhou, H. Qin, Y. Wang and Y. Zhang, 2011. Environmental/economic dispatch problem of power system by using an enhanced multi-objective differential evolution algorithm. Energ. Convers. Manage., 52: 1175-1183.

Mendis, N., K.M. Muttaqi, S. Sayeef and S. Perera, 2012. Standalone operation of wind turbine-based variable speed generators with maximum power extraction capability. IEEE T. Energ. Convers., 27: 822-834.

Mohseni, M., S. Islam and M.A.S. Masoum, 2011. Fault ride-through capability enhancement of doubly-fed induction wind generators. IET Renew. Power Gen., 5: 368-376.

Moutis, P., S.A. Papathanassiou and N.D. Hatziargyriou, 2012. Improved load-frequency control contribution of variable speed variable pitch wind generators. Renew. Energ., 48: 514-523.

Muljadi, E. and C.P. Butterfield, 2001. Pitch-controlled variable-speed wind turbine generation. IEEE T. Ind. Appl., 37: 240-246.

Muyeen, S.M., A. Al-Durra and J. Tamura, 2011. Variable speed wind turbine generator system with current controlled voltage source inverter. Energ. Convers. Manage., 52: 2688-2694.

Qin, H., J. Zhou, Y. Lu, Y. Wang and Y. Zhang, 2010. Multi-objective differential evolution with adaptive Cauchy mutation for short-term multi-objective optimal hydro-thermal scheduling. Energ. Convers. Manage., 51: 788-794.

Qu, L. and W. Qiao, 2011. Constant power control of DFIG wind turbines with super capacitor energy storage. IEEE T. Ind. Appl., 47: 359-367.

Rahim, A.H.M.A. and I.O. Habiballah, 2011. DFIG rotor voltage control for system dynamic performance enhancement. Electr. Pow. Syst. Res., 81: 503-509.

Rahim, A.H.M.A. and E.P. Nowicki, 2012. Supercapacitor energy storage system for fault ride-through of a DFIG wind generation system. Energ. Convers. Manage., 59: 96-102.

Riziotis, V.A., E.S. Politis, S.G. Voutsinas and P.K. Chaviaropoulos, 2008. Stability analysis of pitch-regulated, variable-speed wind turbines in closed loop operation using a linear Eigen value approach. Wind Energ., 11: 517-535.

Senjyu, T., R. Sakamoto, N. Urasaki, T. Funabashi, H. Fujita and H. Sekine, 2006. Output power leveling of wind turbine generator for all operating regions by pitch angle control. IEEE T. Energ. Convers., 21: 467-475.

Shi, J., Y. Tang, Y. Xia, L. Ren and J. Li, 2011. SMES based excitation system for doubly-fed induction generator in wind power application. IEEE T. Appl. Supercon., 21: 1105-1108.

Slowik, A., 2011. Application of an adaptive differential evolution algorithm with multiple trial vectors to artificial neural network training. IEEE T. Ind. Electr., 58: 3160-3167.

Suresh, S., 2009. Adaptive neural flight control system for helicopter. Proceeding of the IEEE Symposium on Computational Intelligence for Security and Defense Applications, pp: 1-8.

Vinothkumar, K. and M.P. Selvan, 2011. Novel scheme for enhancement of fault ride-through capability of doubly fed induction generator based wind farms. Energ. Convers. Manage., 52: 2651-2658.

Xu, T., X. Liu and X. Yang, 2012. A novel approach for ship trajectory online prediction using BP neural network algorithm. Adv. Inform. Sci. Serv. Sci., 4: 271-277.

Yilmaz, A.S. and Z. Ozer, 2009. Pitch angle control in wind turbines above the rated wind speed by multi-layer perceptron and radial basis function neural networks. Expert Syst. Appl., 36: 9767-9775.

Yunus, A.M.S., M.A.S. Masoum and A. Abu-Siada, 2012. Application of SMES to enhance the dynamic performance of DFIG during voltage sag and swell. IEEE T. Appl. Supercon., 22: 5702009.

Zhang, Z.S., Y.Z. Sun, J. Lin and G.J. Li, 2012. Coordinated frequency regulation by doubly fed induction generator-based wind power plants. IET Renew. Power Gen., 6: 38-47.